OPEN ACCESS
JOURNAL OF ADVANCED DIELECTRICS
Vol. 12, No. 3 (2022) 2250007 (7 pages)

DOI: 10.1142/S2010135X22500072

Enhanced ferroelectric and piezoelectric characteristics in Ca-substituted $BaTi_{0.88}Zr_{0.12}O_3$ ceramics

S. B. Chen, S. Y. Wu*,‡ and X. M. Chen†,‡
School of Materials Science and Engineering
Zhejiang University, 38 Zheda Road
Hangzhou 310027, P. R. China
*wushuya@zju.edu.cn
†xmchen59@zju.edu.cn

Received 13 August 2021; Revised 24 April 2022; Accepted 5 May 2022; Published 14 July 2022

In this work, $Ba_{1-x}Ca_xTi_{0.88}Zr_{0.12}O_3$ (x = 0.00–0.25) ceramics were prepared by a solid-state reaction method, and the variation of dielectric, ferroelectric and piezoelectric characteristics has been investigated together with the structure evolution. The crystal structure varies from rhombohedral to tetragonal at room-temperature and the morphotropic phase boundary (MPB) is determined around x = 0.10, where the significantly enhanced ferroelectric and piezoelectric properties are achieved. With the increase of Ca content, the system gradually evolves into a relaxor ferroelectric. This work provides useful guidance for future research on lead-free piezoelectric materials.

Keywords: Morphotropic phase boundary; relaxor ferroelectric; piezoelectric properties.

1. Introduction

For a long time, lead zirconate titanate (PZT) is the dominant piezoelectric material system for electromechanical devices such as actuators, sensors and transducers. However, the increasing success of PZT releases more and more lead into the environment.[1] In recent years, the research of lead-free piezoelectric ceramics to replace PZT has attracted much attention as the concerns about global environment. $BaTiO_3$-based system is one of the most promising candidates as the excellent properties. From a scientific view, the phase diagrams of $BaTiO_3$-based materials involve phase transitions at relatively low temperature, and their functional properties are sensitive both to microstructure and chemical modifications. These reasons make them attractive for probing mechanisms of enhanced piezoelectricity.[2,3] Chemical substitution on the A- and/or B-sites is one of the most effective strategies to modify and improve properties of $BaTiO_3$-based ceramics.

For B-site chemical substitution, $BaZr_xTi_{1-x}O_3$ ceramics have been extensively researched.[4–8] Zr-substitution decreases the Curie temperature, while increases the transition temperatures of R-O and O-T phase transitions. As a result, a morphotropic phase boundary (MPB) appears around x = 0.12, which significantly improves the dielectric, piezoelectric and ferroelectric properties. Meanwhile, the system varies from normal ferroelectric to diffused and relaxor ferroelectric, and finally paraelectric. On the other hand, for A-site substitution, Ca-substitution will lead to the enhancement of dielectric, piezoelectric and ferroelectric characteristics in $Ba_{1-x}Ca_xTiO_3$ ceramics, where the Curie temperature is almost unchanged and the transition temperatures of R-O and O-T phase transitions decrease continuously with increasing Ca-contents.[9,10] The system keeps the normal ferroelectric nature until solid solution limit. For A- and B-site co-substitution, $Ba_{1-x}Ca_xTi_{1-y}Zr_yO_3$ ceramics have received much attention because of the excellent properties. In 2009, Ren *et al*. reported a surprisingly high piezoelectric coefficient of d_{33} = 620 pC/N in $Ba(Ti_{0.8}Zr_{0.2})O_3$-$(Ba_{0.7}Ca_{0.3})TiO_3$ ceramic, which even exceeded that of some PZT ceramics.[10] Since then, many researchers have paid much attention to $Ba_{1-x}Ca_xTi_{1-y}Zr_yO_3$ ceramics, and great progress has been achieved, making the present system a promising candidate for piezoelectric application.[12–16]

Compared with $BaTi_{1-x}Zr_xO_3$ ceramics, the piezoelectric properties of $Ba_{1-x}Ca_xTi_{1-y}Zr_yO_3$ ceramics are significantly improved. By surveying the reported literatures, it can be inferred that Ca-substitution on $BaTi_{1-x}Zr_xO_3$ ceramics might show interesting structure evolution, and excellent properties could be expected. However, most of the research focused on B-site substitution in the present system, and only a few papers have reported the influence of Ca-substitution on electrical properties. Besides, most of them focused on the low Zr concentration.[17–21] Little attention has been paid to Ca-substitution around MPB in $BaTi_{1-x}Zr_xO_3$ ceramics, and the structure and properties evolution are interesting and

‡Corresponding authors.

necessary to be investigated. In this work, effects of Ca substitution upon structure and properties of $BaTi_{0.88}Zr_{0.12}O_3$ ferroelectric ceramics are intensively investigated, and the enhanced dielectric, ferroelectric and piezoelectric properties are determined.

2. Experimental Procedure

$Ba_{1-x}Ca_xTi_{0.88}Zr_{0.12}O_3$ (x = 0, 0.05, 0.1, 0.15, 0.2, 0.25) ceramics were prepared by a standard solid state reaction process, using $BaCO_3$ (99.99%), $CaCO_3$ (99.99), ZrO_2 (99%) and TiO_2 (99.99%) powder as the raw materials. The corresponding raw materials were mixed and ball milled with ZrO_2 media in alcohol for 24 h, and then calcined at 1273–1473 K in air after drying. The calcined powders were re-milled and then pressed into disks under a uniaxial pressure about 98 MPa with 10% polyvinyl alcohol (PVA) as binder. The disks were heated at 873 K for 2 h in air to decompose PVA and finally sintered at 1623–1773 K in air for 3 h to yield dense ceramics. The ceramic is cylinder with a diameter of about 10 mm and a thickness of 1 mm, and the electrode covers its upper and lower circular end faces.

Microstructures of the present ceramics were observed by a field emission scanning electron microscopy (Gemini SEM 300, Zeiss, Oberkochen, Germany) on the thermally etched surfaces. Energy dispersive spectroscopy (EDS) were used to observe element distribution. Crystal structures were identified by powder X-ray diffraction (XRD) with Cu Kα radiation (Bruker D8 Advance, Bruker, Karlsruhe, Germany) at room temperature. The data for Rietveld analysis were collected over the 2θ range 10°–130° at a step width of 0.02°, and the Rietveld structure refinement were carried out by the FullProf program. The dielectric measurement was carried out with a broad dielectric spectrometer (Turnkey Concept 50, Novocontrol Technologies, Hundsangen, Germany) in a wide temperature range (from 243 K to 473 K) at frequencies from 100 Hz to 1 MHz. Silver electrodes were used for the dielectric measurement. The room temperature polarization–electric field (P-E) hysteresis loops were measured using a Precision Materials Analyzer (RT Premier II, Radiant Technologies Inc, Albuquerque, NM). Gold was sputtered on the surfaces of the present ceramics as the electrodes, and all the samples were immersed in silicon oil during measurement to prevent possible air breakdown at a high field. The piezoelectric properties were measured at room temperature by using a quasi-static d_{33} piezometer (ZJ-3A, IACAS, Beijing, China).

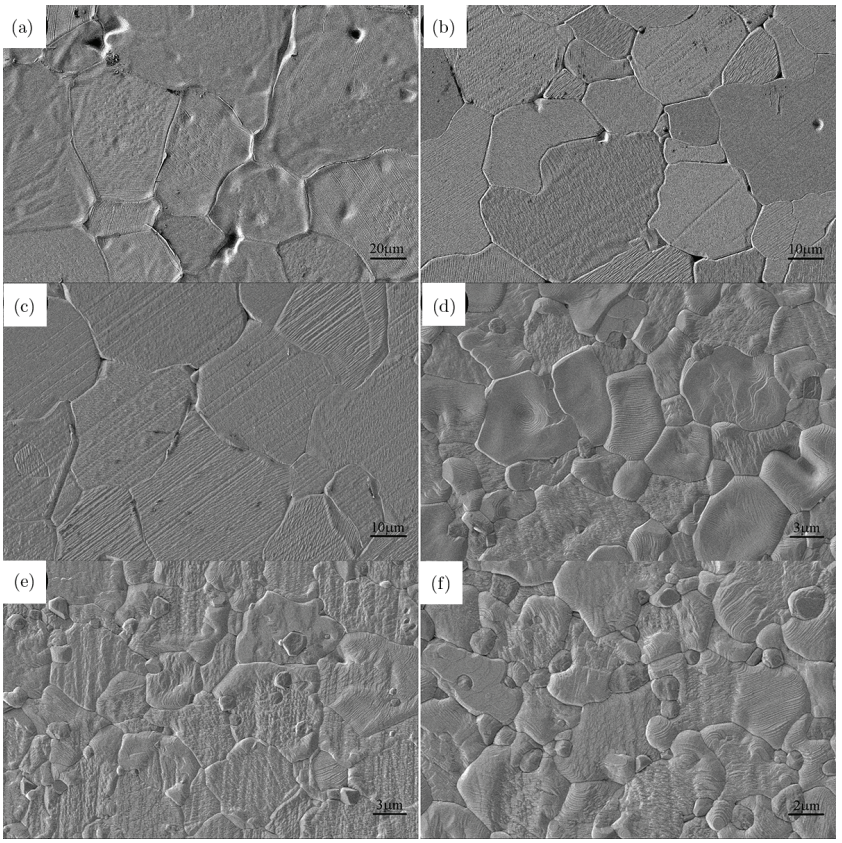

Fig. 1. SEM photographs of thermally etched surface of $Ba_{1-x}Ca_xTi_{0.88}Zr_{0.12}O_3$ ceramics: (a) x = 0, (b) x = 0.05, (c) x = 0.10, (d) x = 0.15, (e) x = 0.20, (f) x = 0.25.

3. Results and Discussion

As shown in Fig. 1, dense $Ba_{1-x}Ca_xTi_{0.88}Zr_{0.12}O_3$ ceramics with homogeneous fine microstructure are obtained for all compositions investigated. As shown in Table 2, x increases and the average grain size decreases. Besides, the grain size of the present ceramics with $x = 0$–0.1 is uniform, while that with $x = 0.15$–0.25 has a large difference. There are many small grains distributed between larger ones when $x \geq 0.15$. This is related to the component reaching the solid solution limit, and secondary phase appears when $x \geq 0.15$. In order to verify the occurrence of secondary phase, all compositions were characterized by back scattered electron images and EDS spectrum was carried out at the same time. The results are shown in supplementary material. The backscattered electron image and EDS spectrum show that the solid solution limit of the present system is around $x = 0.15$.

The fitting results of crystal structure of $Ba_{1-x}Ca_xTi_{0.88}Zr_{0.12}O_3$ ceramic at room temperature are shown in Fig. 2 and Table 1. The major phase of all compositions is perovskite structure. No miscellaneous phases are found when $x \leq 0.1$; while in the composition of $x = 0.15$, there are a few miscellaneous peaks, but they are difficult to distinguish from the background signal; for the composition of $x = 0.2$ and $x = 0.25$, there are 3.1% and 7.9% of the miscellaneous phases, respectively. It can be determined by the full spectrum fitting that the impurity phase is the orthorhombic phase $CaTiO_3$ and the space group is *Pbnm*. This means the solid

Table 1. Refined parameters for $Ba_{1-x}Ca_xTi_{0.88}Zr_{0.12}O_3$ ceramics from XRD data.

	$x = 0$	$x = 0.05$	$x = 0.10$
Unit cell (R)	$a = b = 5.6988$ Å $c = 6.9876$ Å	$a = b = 5.6946$ Å $c = 6.9746$ Å	$a = b = 5.6839$ Å $c = 6.9586$ Å
Unit cell (T)			$a = b = 4.0118$ Å $c = 4.0385$ Å
Crystal system	Rhombohedral	Rhombohedral	Tetragonal (87.9%) + Rhombohedral (12.1%)
Reliability factors	$R_{exp} = 5.39\%$ $R_{wp} = 11.9\%$ $R_p = 8.54\%$ $\chi^2 = 4.85$	$R_{exp} = 4.74\%$ $R_{wp} = 10.4\%$ $R_p = 7.66\%$ $\chi^2 = 4.81$	$R_{exp} = 5.33\%$ $R_{wp} = 10.5\%$ $R_p = 7.67\%$ $\chi^2 = 3.86$
	$x = 0.15$	$x = 0.20$	$x = 0.25$
Unit cell (T)	$a = b = 4.0088$ Å $c = 4.0174$ Å	$a = b = 4.0090$ Å $c = 4.0134$ Å	$a = b = 4.0102$ Å $c = 4.0166$ Å
Crystal system	Tetragonal (99.1%) + Secondary phase (0.9%)	Tetragonal (96.9%) + Secondary phase (3.1%)	Tetragonal (92.1%) + Secondary phase (7.9%)
Reliability factors	$R_{exp} = 6.14\%$ $R_{wp} = 10.4\%$ $R_p = 7.79\%$ $\chi^2 = 2.88$	$R_{exp} = 6.31\%$ $R_{wp} = 10.4\%$ $R_p = 7.55\%$ $\chi^2 = 2.73$	$R_{exp} = 6.13\%$ $R_{wp} = 11.0\%$ $R_p = 8.49\%$ $\chi^2 = 3.22$

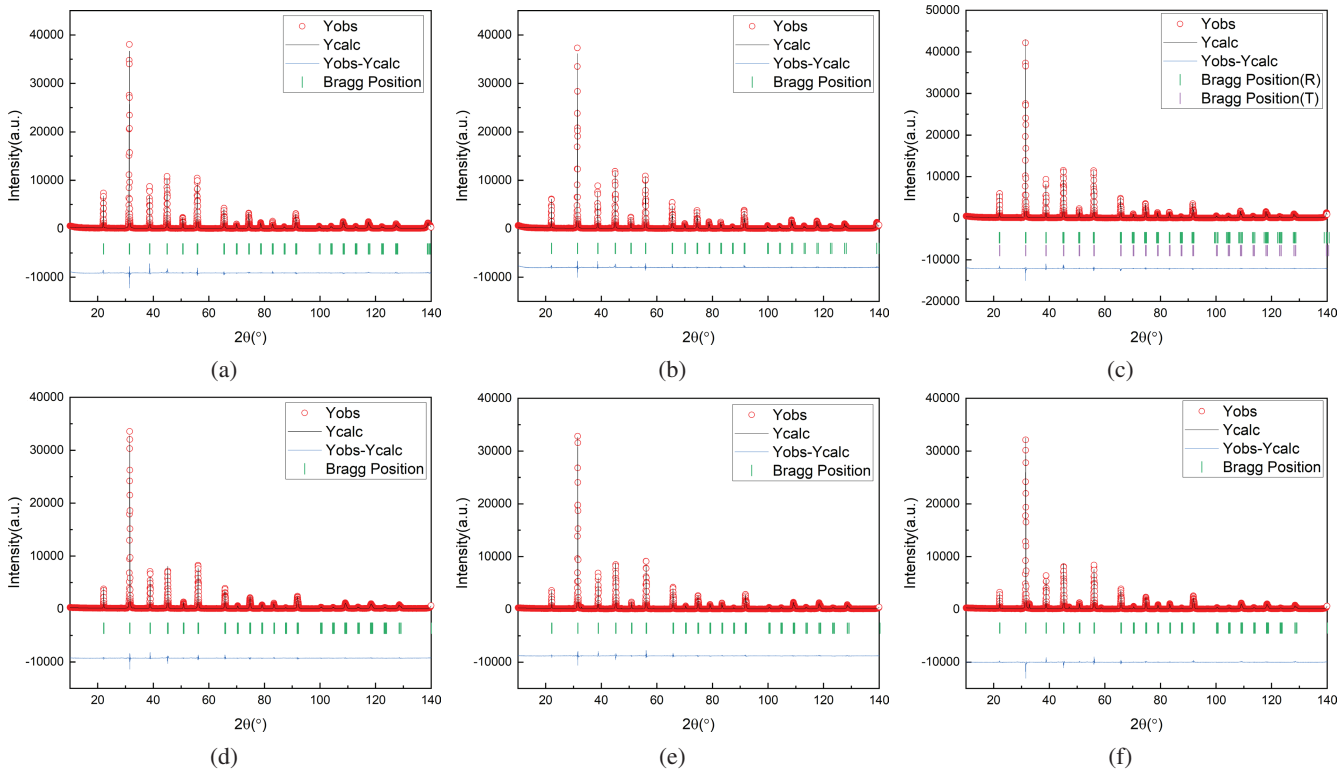

Fig. 2. (Color online) Rietveld analysis results of XRD patterns for $Ba_{1-x}Ca_xTi_{0.88}Zr_{0.12}O_3$ ceramics: (a) $x = 0$, (b) $x = 0.05$, (c) $x = 0.10$, (d) $x = 0.15$, (e) $x = 0.20$, (f) $x = 0.25$ (Experiment data: Red circles; Calculated data: Black lines; Difference: Blue lines).

solution limit of the present system is near $x = 0.15$, which is consistent with previous analysis. In the end member of the present system, $BaTi_{0.88}Zr_{0.12}O_3$, three phase transition temperatures of cubic-tetragonal, tetragonal-orthogonal and orthogonal-rhombic converge to form an MPB. At room temperature, the crystal structure of $BaTi_{0.88}Zr_{0.12}O_3$ ceramic is rhombohedral phase. Refinement results show that with the increase of x, the room temperature phase structure gradually evolves from rhombohedral phase to tetragonal phase and the miscellaneous phase occurs in the composition of $x = 0.15$. At the same time, as x increases, the unit cell parameters of the tetragonal and rhombohedral phases gradually decrease, but almost remain unchanged after solid solution limit, which is related to the ionic radius. The radius of Ca ions is smaller than that of Ba ions. With the increase of x, the content of Ca increases, so the unit cell parameters decrease;

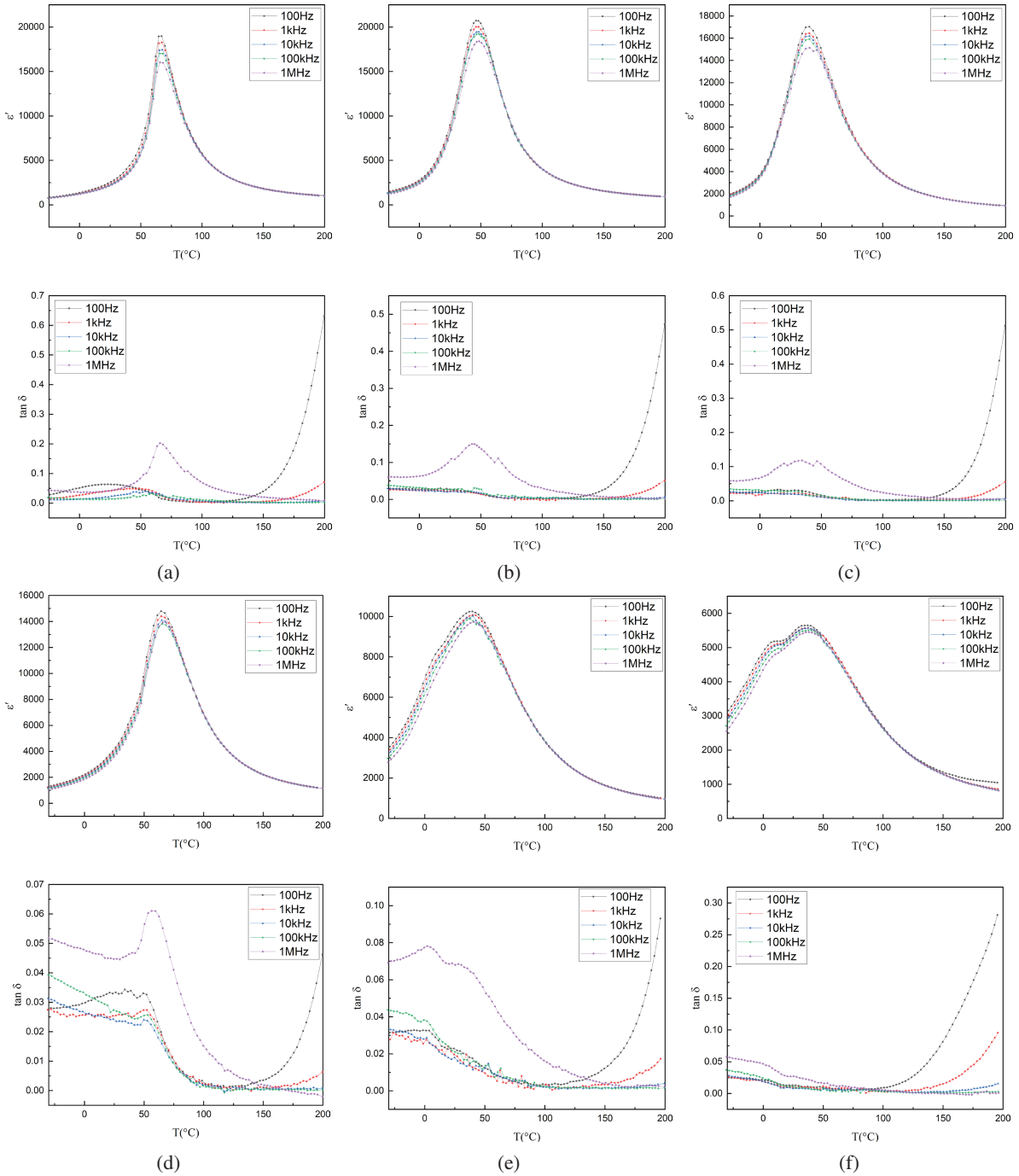

Fig. 3. Temperature dependences of dielectric constant ($\varepsilon'(T)$) and dielectric loss ($\tan\delta(T)$) for $Ba_{1-x}Ca_xTi_{0.88}Zr_{0.12}O_3$ ceramics: (a) $x = 0$, (b) $x = 0.05$, (c) $x = 0.1$, (d) $x = 0.15$, (e) $x = 0.15$, (f) $x = 0.2$ measured at −30–200°C.

Table 2. The change of the average grain size with the content of Ca^{2+}.

x	0	0.05	0.1	0.15	0.2	0.25
Average grain size (μm)	48.3	25.3	19.7	5.4	5.0	2.8

after the solid solution phenomenon, Ca ions do not enter the perovskite structure lattice, so the unit cell parameters are almost maintained constant.

Figure 3 shows the dielectric temperature spectrum of $Ba_{1-x}Ca_xTi_{0.88}Zr_{0.12}O_3$ ceramics during the heating process. It can be seen that when $x \le 0.1$, only one dielectric peak can be observed in the dielectric temperature spectrum, while when $x \ge 0.15$, there is a shoulder peak near the major peak of the dielectric anomaly. This indicates that the phase transitions converged in the end member and gradually disperse with the increase of x. Besides, when $x = 0$, the dielectric anomaly peak is very sharp; with the increase of x, the dielectric anomaly peak gradually broadens, and there is a slight frequency dispersion phenomenon in the compositions of $x \ge 0.2$, indicating that the system transforms to relaxor. In other words, with the increase of x, the phase transition dispersion gradually increases, and finally evolves into a relaxor ferroelectric.

The modified Curie–Weiss law can describe the ferroelectric phase transition dispersion well.

$$\frac{1}{\varepsilon'} - \frac{1}{\varepsilon'_m} = \frac{(T - T_m)^\gamma}{C}, \quad (1)$$

where ε'_m is the peak value of ε', C is a constant and γ is the degree of relaxation, evaluating the diffuse degree of phase transition. $\gamma = 1$ means it is a normal Curie–Weiss transition, while $\gamma = 2$ means it is a complete relaxor transition.[21] As shown in Fig. 4, the linearity of the fit is quite good. With the increase of x, the degree of relaxation γ increases monotonously: when $x = 0$, $\gamma = 1.54$; when $x \ge 0.2$, the degree of relaxation γ is close to 2, which is close to that of the standard relaxor ferroelectric. The variation of degree of relaxation is consistent with the appearance of slight frequency dispersion in the dielectric temperature spectrum. According to these results, it can be judged that as x increases, the phase transition dispersion of the system gradually increases, and finally evolves into relaxor ferroelectric.

It is generally considered that the relaxor ferroelectric phenomenon originates from the heterogeneous microstructure.[22] In the $BaTi_{1-x}Zr_xO_3$ system, the heterogeneous microstructure is due to the random distribution of Zr^{4+} and Ti^{4+} on B-site. Zr^{4+} and Ti^{4+} have different ion radius, which leads to a random stress field; in addition, many studies have shown that Zr^{4+} is completely located in the center of the oxygen octahedron, while Ti^{4+} has a displacement away from the oxygen octahedron. The random distribution of Ti^{4+} and Zr^{4+} will cause a heterogeneous chemical environment.[4] Therefore, in the $BaTi_{1-x}Zr_xO_3$ system, as the amount of Zr substitution increases, the system evolves into relaxor. On the other hand, the substitution of Ca on the A-site has little effect on the relaxation evolution. In the $Ba_{1-x}Ca_xTiO_3$ system, although the degree of phase transition dispersion increases with the increase of Ca substitution, there is no frequency dispersion phenomenon until the solid solution limit ($x = 0.25$) is reached.[9] In this work, the amount of Zr substitution on the B site remains unchanged. With the increase of Ca substitution, the system gradually evolves into a relaxor ferroelectric. It is worth noticing that in the $BaTi_{1-x}Zr_xO_3$ system, the amount of Zr substitution required for frequency dispersion is usually more than 0.25;[3] in this work, the amount of Zr substitution is only 0.12, which means that the Ca substitution on A-site promotes the relaxation evolution of the present system. The possible reason may be that the ion radius of Ba^{2+} and Ca^{2+} are quite different, and their random distribution enhances the

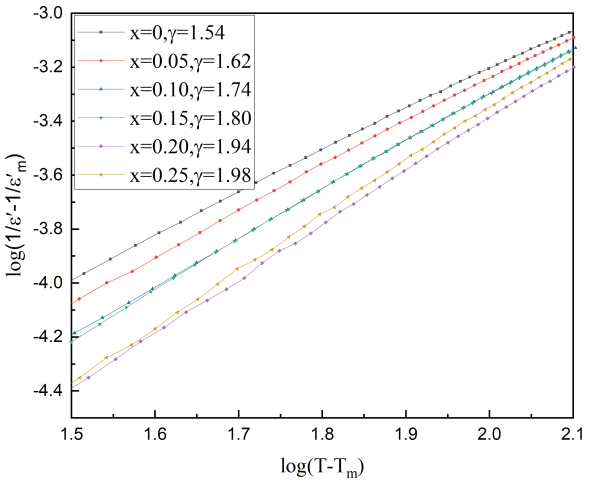

Fig. 4. Plots of $\log(1/\varepsilon' - 1/\varepsilon_m)$ versus $\log(T - T_m)$ at 100 kHz for $Ba_{1-x}Ca_xTi_{0.88}Zr_{0.12}O_3$ ceramics ($x = 0$, 0.05, 0.1, 0.15, 0.20, 0.25).

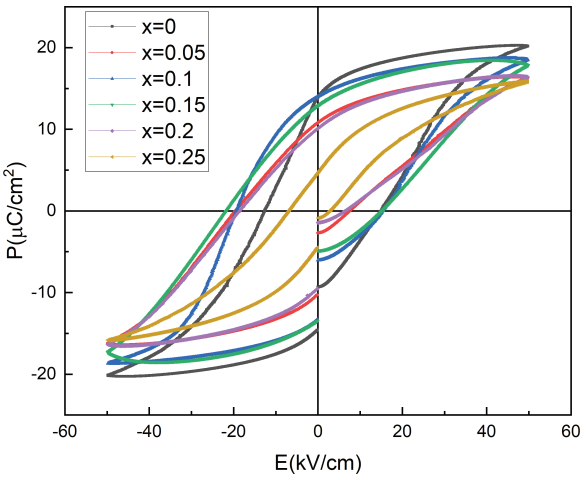

Fig. 5. *P-E* curves measured at room temperature with a triangular wave form at 10 Hz for $Ba_{1-x}Ca_xTi_{0.88}Zr_{0.12}O_3$ ceramics ($x = 0$, 0.05, 0.1, 0.15, 0.20 and 0.25).

Table 3. The values of P_{max} and P_r vary with the content of Ca^{2+}.

x	0	0.05	0.1	0.15	0.2	0.25
P_r (μC/cm^2)	14.3	10.6	13.7	13.2	9.8	4.6
P_m (μC/cm^2)	20.3	16.4	18.6	18.5	16.4	15.3

random stress field of the system, so only a smaller amount of Zr substitution is sufficient to make the system evolve into a relaxor ferroelectric.

The hysteresis loop of $Ba_{1-x}Ca_xTi_{0.88}Zr_{0.12}O_3$ ceramic at room temperature is shown in Fig. 5. The values of P_{max} and P_r vary with the content of Ca^{2+} are listed in Table 3. When $x = 0$, it is a typical saturated hysteresis loop; as x increases to $x = 0.05$, the remanent polarization decreases, and the ferroelectricity is weakened. This is because the smaller radius of Ca^{2+} ions replace Ba^{2+} ions, which reduces the oxygen octahedral gap in the unit cell, and the spontaneous displacement of Ti^{4+} ions decrease; and as x continues to increase, around $x = 0.10$, the composition is close to the MPB of the system. As a result, the polarization reversal barrier is reduced, and the ferroelectricity is enhanced, which is close to the composition of $x = 0$. When x further increases to $x = 0.2$, the composition deviates from the MPB, and the ferroelectricity weakens, which is closer to the composition of $x = 0.05$. When x increases to 0.25, the ion size effect further weakens the ferroelectricity, and the remanent polarization and coercive field reduces. Besides, as x increases, the shape of the hysteresis loop changes significantly. The composition of $x = 0$ is the saturated hysteresis loop, while that of $x = 0.25$ is the slender hysteresis loop, which is the characteristic of relaxor ferroelectrics. The evolution of the shape of the hysteresis loop further confirms that the system gradually evolved into a relaxor ferroelectric with the increase of Ca substitution.

The evolution of the piezoelectric constant d_{33} with the composition of $Ba_{1-x}Ca_xTi_{0.88}Zr_{0.12}O_3$ ceramics at room temperature is shown in Fig. 6. When $x = 0$, d_{33} is about 212 pC/N, which is very close to that reported in the literature;[6] with the increase of x, the piezoelectric constant d_{33} gradually increases. On the composition near the MPB $x = 0.1$, the maximum value is obtained, 422 pC/N. This is because the free energy curve of the system becomes smooth, and the free energy barrier between different polarization directions is close to zero near the MPB. As a result, the polarization is easy to flip, which significantly improves the piezoelectric performance. With the further increase of x, the composition deviates from the MPB, and the piezoelectric constant d_{33} decreases. But unlike the B-site Zr substitution, the system has not evolved into a paraelectric phase until $x = 0.25$, so the piezoelectricity has not disappeared.

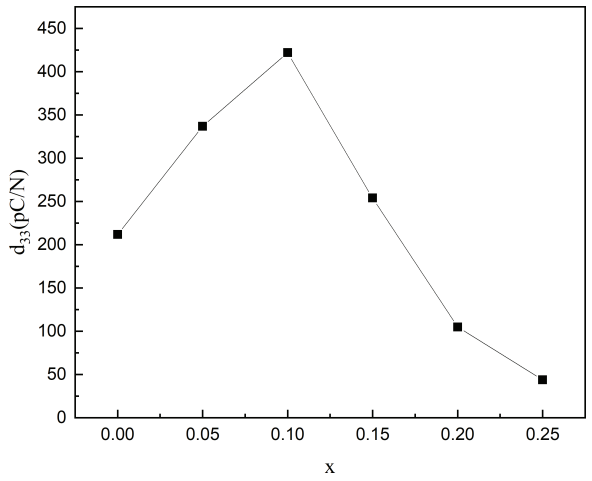

Fig. 6. Piezoelectric coefficients d_{33} of $Ba_{1-x}Ca_xTi_{0.88}Zr_{0.12}O_3$ ceramics: $x = 0$, $x = 0.05$, $x = 0.1$, $x = 0.15$, $x = 0.20$ and $x = 0.25$.

4. Conclusions

$Ba_{1-x}Ca_xTi_{0.88}Zr_{0.12}O_3$ ceramics were synthesized by a standard solid state reaction method. The solubility limit lies around $x = 0.15$ for the present ceramics. XRD study indicates that the crystal structure evolves from rhombohedral phase to tetragonal phase, and there is an MPB around $x = 0.1$. Near MPB composition, the dielectric, ferroelectric and piezoelectric properties are significantly enhanced as the polarization anisotropy almost vanishes. The system gradually evolved into a relaxor ferroelectric with the increase of Ca substitution. The enhanced piezoelectric properties were obtained at the composition of $x = 0.1$ ($d_{33} \sim 422$ pC/N at room temperature) for the present ceramics, which might provide useful guidance for the future research on lead-free piezoelectric materials.

Acknowledgments

This work was financially supported by National Natural Science Foundation of China under Grant No. 51790493.

References

[1]J. Rödel, W. Jo, K. T. P. Seifert, E. M. Anton, T. Granzow and D. Damjanovic, Perspective on the development of lead-free piezoceramics, *J. Am. Ceram. Soc.* **92**, 1153 (2009).

[2]M. Acosta, N. Novak, V. Rojas, S. Patel, R. Vaish, J. Koruza, G. A. Possetti and J. Rödel, $BaTiO_3$-based piezoelectrics: Fundamentals, current statue, and perspectives, *Appl. Phys. Rev.* **4**, 041305 (2017).

[3]T. Wang, J. C. Hu, H. B. Yang, L. Jin, X. Y. Wei, C. C. Li, F. Yan and Y. Lin, Dielectric relaxation and Maxwell–Wagner interface polarization in Nb_2O_5 doped $0.65BiFeO_3$–$0.35BaTiO_3$ ceramics, *J. Appl. Phys.* **121**, 084103 (2017).

[4]T. Maiti, R. Guo and A. S. Bhalla, Structure–property phase diagram of $BaZr_xTi_{1-x}O_3$ system, *J. Am. Ceram. Soc.* **91**, 1769 (2008).

[5]L. Dong, D. S. Stone and R. S. Lakes, Enhanced dielectric and piezoelectric properties of $x BaZrO_3$-$(1-x)BaTiO_3$ ceramics, *J. Appl. Phys.* **111**, 084107 (2012).

[6]A. K. Kalyani, A. Senyshyn and R. Ranjan, Polymorphic phase boundaries and enhanced piezoelectric response in extended composition range in the lead free ferroelectric $BaTi_{1-x}Zr_xO_3$, *J. Appl. Phys.* **114**, 014102 (2013).

[7]Z. Yu, C. Ang, R. Guo and A. S. Bhalla, Piezoelectric and strain properties of $Ba(Ti_{1-x}Zr_x)O_3$ ceramics, *J. Appl. Phys.* **92**, 1489 (2002).
[8]A. K. Kalyani, A. Senyshyn and R. Ranjan, Polymorphic phase boundaries and enhanced piezoelectric response in extended composition range in the lead free ferroelectric BaTi1-xZrxO3, *J. Appl. Phys.* **114**, 014102 (2013).
[9]X. N. Zhu, W. Zhang and X. M. Chen, Enhanced dielectric and ferroelectric characteristics in Ca-modified $BaTiO_3$ ceramics, *AIP Adv.* **3**, 082125 (2013).
[10]D. Fu, M. Itoh, S. Y. Koshihara, T. Kosugi and S. Tsuneyuki, Anomalous phase diagram of ferroelectric $(Ba,Ca)TiO_3$ single crystals with giant electromechanical response, *Phys. Rev. Lett.* **100**, 227601 (2008).
[11]W. Liu and X. B. Ren, Large piezoelectric effect in Pb-free ceramics, *Phys. Rev. Lett.* **103**, 257602 (2009).
[12]D. Xue, Y. Zhou, H. Bao, C. Zhou, J. Gao and X. B. Ren, Elastic, piezoelectric, and dielectric properties of $Ba(Zr_{0.2}Ti_{0.8})$-O_3-50$(Ba_{0.7}Ca_{0.3})TiO_3$ Pb-free ceramic at the morphotropic phase boundary, *J. Appl. Phys.* **109**, 054110 (2011).
[13]D. S. Keeble, F. Benabdallah, P. A. Thomas, M. Maglione and J. Kreisel, Revised structural phase diagram of $(Ba_{0.7}Ca_{0.3}TiO_3)$-$(BaZr_{0.2}Ti_{0.8}O_3)$, *Appl. Phys. Lett.* **102**, 092903 (2013).
[14]Y. Zhang, G. Sun and W. Chen, A brief review of $Ba(Ti_{0.8}Zr_{0.2})$-O_3-$(Ba_{0.7}Ca_{0.3})TiO_3$ based lead-free piezoelectric ceramics: Past, present and future perspectives, *J. Phys. Chem. Solids* **114**, 207 (2018).
[15]M. Sutapun, T. Charoonsuk, T. Kolodiazhnyi and N. Vittayakorn, $CaTiO_3$ induced ferroelectric phase coexistence and low temperature dielectric relaxation in $BaTiO_3$-$BaZrO_3$ ceramics, *J. Am. Ceram. Soc.* **101**, 1957 (2018).
[16]Y. Huang, C. Zhao, X. Lv, H. Wang and J. Wu, Multiphase coexistence and enhanced electrical properties in (1-*x*-*y*) $BaTiO_3$-*x*Ca-TiO_3-*y*$BaZrO_3$ lead-free ceramics, *Ceram. Int.* **143**, 13516 (2017).
[17]X. Nie, S. G. Yan, S. B. Guo, F. Gao, C. H. Yao, C. L. Mao, X. L. Dong and G. S. Wang, Influence of Ca^{2+} concentration on structure and electrical properties of $(Ba_{1-x}Ca_x)(Zr_{0.2}Ti_{0.8})O_3$ ceramics, *Mater. Res. Express* **5**, 036301 (2018).
[18]T. Mondal, S. Das, T. Badapanda, T. P. Sinha and P. M. Sarun, Effect of Ca^{2+} substitution on impedance and electrical conduction mechanism of $Ba_{1-x}Ca_xZr_{0.1}Ti_{0.9}O_3$ ($0.00 \leq x \leq 0.20$) ceramics, *Physica B* **508**, 124 (2017).
[19]N. Pisitpipathsin, P. Kantha, K. Pengpat and G. Rujijanagul, Influence of Ca substitution on microstructure and electrical properties of $Ba(Zr,Ti)O_3$ ceramics, *Ceram. Int.* **39**, S35 (2013).
[20]W. Li, A. J. Xu, R. Q. Chu, P. Fu and G. Z. Zang, Structural and dielectric properties in the $(Ba_{1-x}Ca_x)(Ti_{0.95}Zr_{0.05})O_3$ ceramics, *Curr. Appl. Phys.* **12**, 748 (2012).
[21]W. Li, A. J. Xu, R. Q. Chu, P. Fu and G. Z. Zang, Polymorphic phase transition and piezoelectric properties of $(Ba_{1-x}Ca_x)$-$(Ti_{0.9}Zr_{0.1})O_3$ lead-free ceramics, *Physica B* **405**, 4513 (2010).
[22]V. V. Shvartsman, D. C. Lupascu and D. J. Green, Lead-free relaxor ferroelectrics, *J. Am. Ceram. Soc.* **95**, 1 (2012).